



# How Dense of a Circumstellar Medium Is Sufficient to Choke a Jet?

Paul C. Duffell<sup>1</sup> and Anna Y. Q. Ho<sup>2</sup> <sup>1</sup>Harvard-Smithsonian Center for Astrophysics, 60 Garden Street, Cambridge MA 02138, USA; [paul.duffell@cfa.harvard.edu](mailto:paul.duffell@cfa.harvard.edu)<sup>2</sup>California Institute of Technology, 1200 E. California Boulevard, Pasadena CA 91125, USA

Received 2019 July 6; revised 2020 July 16; accepted 2020 July 22; published 2020 September 15

## Abstract

The progenitor stars of stripped-envelope high-velocity supernovae (Ic-BL SNe) can explode inside a dense circumstellar medium (CSM) that extends out to many times the progenitor radius. This complicates the question of whether all Ic-BL SNe harbor a jet, which can tunnel through the star and be viewed on-axis as a long-duration gamma-ray burst (GRB). More specifically, a sufficiently dense CSM might “choke” the jet, redistributing its energy quasi-spherically. In this study, we numerically calculate the CSM density necessary for jet choking. For typical GRBs, we determine the jet is not choked in the CSM unless  $\rho r^2 > 4 \times 10^{19} \text{ g cm}^{-1}$ ; this requires several solar masses of CSM to be situated within  $10^{13} \text{ cm}$  of the progenitor, a much higher density than any CSM observed. We conclude that typical GRB jets are not choked in the CSM. However, in many cases the CSM has sufficient mass to decelerate the jet to a modest Lorentz factor ( $\Gamma \sim 10$ ), which should lead to a long coasting phase for the jet, observable as a long plateau (potentially up to a few days) in the afterglow light curve. For extreme cases of low-energy GRBs in a high-mass CSM, the jet will decelerate to nonrelativistic velocities, causing it to spread modestly to a larger opening angle ( $\theta_j \approx 20^\circ$ ) before breaking out of the CSM. Even in these extreme examples, the jet does not have time to redistribute its energy quasi-spherically in the CSM before breakout.

*Unified Astronomy Thesaurus concepts:* [Circumstellar matter \(241\)](#); [Supernovae \(1668\)](#); [Relativistic jets \(1390\)](#); [Relativistic fluid dynamics \(1389\)](#); [Gamma-ray bursts \(629\)](#)

## 1. Introduction

In the traditional model of a core-collapse supernova (CC SN), the core collapses and a shock unbinds the star with an energy release of  $\sim 10^{51} \text{ erg}$ . A subset of CC SNe show no evidence for hydrogen and helium in their spectra; these are thought to arise from progenitors that have been stripped of their outer envelopes, and are classified as Type Ic (Filippenko 1997). A subset of SNe Ic are unusually fast and energetic: their photospheric velocities are a factor of two or more larger than typical CC SNe, and their kinetic energies an order of magnitude greater. Their spectral features are also broader than that of typical Ic spectra (Modjaz et al. 2016) giving rise to the classification “broad-lined” Ic (Ic-BL).

The reason for these large energies and high velocities is unknown, but one clue lies in the fact that Ic-BL SNe are the only type of SN ever observed in conjunction with a long-duration gamma-ray burst (GRB; Woosley & Bloom 2006; Cano et al. 2017). In fact, it has been suggested that all Ic-BL SNe harbor a jet, and that a GRB is the unusual case in which the jet successfully tunnels through the star and is viewed on-axis (Sobacchi et al. 2017; Barnes et al. 2018).

Observations of some Ic-BL SNe have shown evidence for high densities in the immediate vicinity of the progenitor star. One line of evidence is double-peaked optical light curves (Piro 2015), with a first peak from interaction and the second peak from the radioactive decay of Ni-56. This was first observed in SN2006aj (Campana et al. 2006), which was inferred to have a circumstellar medium (CSM) mass of  $0.01 M_\odot$  distributed within  $\sim 3 \times 10^{13} \text{ cm}$  (Nakar & Piro 2014). A larger CSM mass can extend the first peak, blending it into the second peak—the result is a light curve too rapidly rising and luminous to be explained by the usual radioactive decay. This was first seen in iPTF16asu (Whitesides et al. 2017) and then again in SN2018gep (Ho et al. 2019).

Another line of evidence is luminous radio and X-ray emission, as in PTF11qj (Corsi et al. 2014), SN2007bg (Salas et al. 2013), and SN2003L (Soderberg et al. 2006). Analysis of GRB afterglow spectra has also pointed toward high-density CSM surrounding their progenitors (Margutti et al. 2015).

Given that GRBs and Ic-BL SNe have been observed to have high-density ambient media, it is worth asking how this environment might alter the dynamics of a GRB jet. In particular, Nakar (2015) posited that a GRB jet would have to be choked in such a dense environment, and that these “choked jets” could explain the class of low-luminosity GRBs that have been observed at low redshift (Nakar 2015) and which could be a source of high-energy neutrinos (Mészáros & Waxman 2001).

In this paper, we define “choked” as follows. As the jet tunnels through the star, the ram pressure in the jet balances with the thermal pressure in the cocoon. When the engine shuts off, the ram pressure is suddenly removed. The high-pressure cocoon then crushes the jet core, contaminating it with baryons and quickly thermalizing the jet kinetic energy. The flow from that point on mostly resembles a nonrelativistic blastwave, which rapidly evolves toward a spherical explosion (Irwin et al. 2019). Jet choking is typically seen in calculations of a jet drilling through a star when the engine is shut off before breakout from the stellar surface (MacFadyen et al. 2001). Here we instead explore the idea of jet choking outside the stellar surface, in the dense CSM.

A distinction is being made here between simple “jet spreading,” which all jets do eventually, and this rapid lateral expansion characterized by a choked jet, as described in Irwin et al. (2019). In this study we choose to define a “choked jet” to mean one which spreads rapidly according to Irwin et al. (2019) as soon as the jet head receives the information that the engine has been shut off. A jet that evolves in this fashion would redistribute its energy into a roughly spherical blastwave

by the time it emerges from the dense CSM surrounding the star.

This idea that jets could be choked in the CSM has been applied to other observations. After observations of a jet cocoon were reported associated with SN2017iuk (Izzo et al. 2019), Nakar (2019) argued that the associated jet would have been choked in the extended CSM. Terreran et al. (2019) speculated that a jet may have been choked in the dense CSM surrounding the energetic SN2016coi.

Nakar (2015) regarded the dense CSM around SN2006aj as an extension of the stellar envelope, meaning that the jet has a much longer distance to propagate before breakout than in normal (stripped) GRB progenitors. In fact, interpreting the CSM in this way almost guarantees that any jet will be choked in this medium, unless the engine is left on for a long enough time. If one assumes a trans-relativistic jet head, one requires the engine to be left on for a light-crossing time, which is

$$t_{\text{engine}} > R_{\text{CSM}}/c \sim 10^3 \text{ s}. \quad (1)$$

However, if the jet head is moving at nearly the speed of light, then one can shut off the engine earlier and still have a successful jet, as the information that the engine is shut off will take some time to catch up with the jet head:

$$t_{\text{engine}} > R_{\text{CSM}}(1/v_j - 1/c) \approx R/(\Gamma^2 c) \sim 10\text{--}100 \text{ s}. \quad (2)$$

Given that typical long-GRB durations are  $\sim 10$  s, it stands to reason that most GRB jets would be choked in such a medium.

However, this cannot be the only criterion for jet choking, as clearly the CSM needs to be above some critical density to be capable of choking the jet. For example, the GRB afterglow jets we observe are in no danger of being “choked” by the ISM in this fashion, even after the engine has long been shut off. One reason for this is due to the relativistic velocities of afterglow jets; for example, if the jet head is moving with a large enough Lorentz factor such that  $\Gamma > 1/\theta$ , causality arguments prevent the jet from choking or spreading at all until it decelerates below this threshold.

This study aims to calculate the critical density necessary for jet choking in the long-GRB context. In Section 2 we argue that this criterion should only depend on the ratio  $L_{\text{iso}}/A$ , where  $L_{\text{iso}}$  is the isotropic equivalent engine luminosity, and  $A = \rho r^2$  is the density parameter assuming the CSM is distributed in a wind profile (if the density profile is not a wind, then the quantity  $\rho r^2$  is evaluated at the position of the jet head at the time the engine shut-off has been communicated to the jet head). In Section 3 we calculate the critical value of  $L_{\text{iso}}/A$  using numerical calculations of a jet breaking out of a star in different CSM environments. Additionally, we calculate how much the CSM decelerates the jet, and whether this deceleration is by itself sufficient to spread the jet significantly. Finally, in Section 4 these results are synthesized and applied to interpretations of observed CSM around SNe.

## 2. Analytical Considerations

In order for a jet to be choked when the engine is turned off, there must be some criterion on the local density. For example, GRB afterglows can persist long after the engine is turned off. In this case, the jet is not being actively collimated by the medium; instead of a “cocoon” there is really just a bow shock, which does not take an active role in collimating the jet. In this case, the jet will only decelerate and spread after it sweeps up sufficient mass.

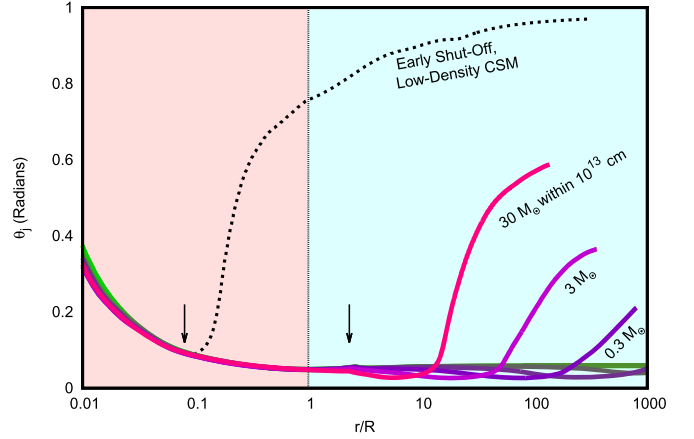


**Figure 1.** Evolution of opening angle  $\theta_j$  of the jet with forward shock radius  $r$  (scaled by stellar radius  $R$ ), for the eight different CSM densities considered. The dashed curve is the “Early Shut-Off” model whose engine is shut off before the jet has escaped the star. All other models have engines that are shut off after breakout from the stellar surface (shut-off times indicated by black arrows); in that case, one requires a very high-density CSM ( $A > 4 \times 10^{19} \text{ g cm}^{-1}$  or  $\lambda < 10$ ) in order to choke the jet.

This situation is distinct from when the engine is still pushing a jet through the progenitor star, because in that case the jet is being collimated by the star. Only after breakout does collimation cease and the opening angle of the jet is given by the opening angle of the engine ( $\theta_j = \theta_0$ ). Therefore, the question of whether the engine turning off will affect the jet should be equivalent to the question of whether the jet is being collimated by the surrounding medium.

This question can be rephrased in the language of Bromberg et al. (2011), which describes various regimes of jet propagation depending on the engine power and ambient density. The relevant condition for a collimated versus uncollimated jet is

$$\tilde{L} \gtrsim \theta_0^{-4/3}, \quad (3)$$

where  $\tilde{L} = L/(\rho t^2 \theta_0^2 c^5)$ . As the jet is relativistic in this regime, one can substitute  $r = ct$ . For a wind medium with  $\rho = A/r^2$ , this is  $\tilde{L} = L/(A \theta_0^2 c^3)$ .

Thus, the condition can be expressed in terms of the quantity  $\lambda$ :

$$\lambda \equiv \frac{L}{A \theta_j^2 c^3}, \quad (4)$$

where  $A = \rho r^2$ , and  $\rho$  and  $r$  are evaluated at the position of the shock front at the time the engine shut-off is communicated to the jet head.

If  $\lambda < \lambda_{\text{crit}}$ , the jet will be choked as soon as the engine is shut off. Bromberg et al. (2011) predict that this  $\lambda_{\text{crit}} \sim \theta_j^{-4/3} \approx 10$ , but we will determine its value for a single choice of the jet opening angle ( $\theta_j = 0.05$ , see Figure 1). In reality,  $\lambda_{\text{crit}}$  should depend on  $\theta_j$ .

## 3. Numerical Calculations

For  $\lambda$  below some critical value, the jet will be choked when the engine shuts off. In this study, we calculate this critical value  $\lambda_{\text{crit}}$  via a direct numerical calculation of a jet breaking out of a star.

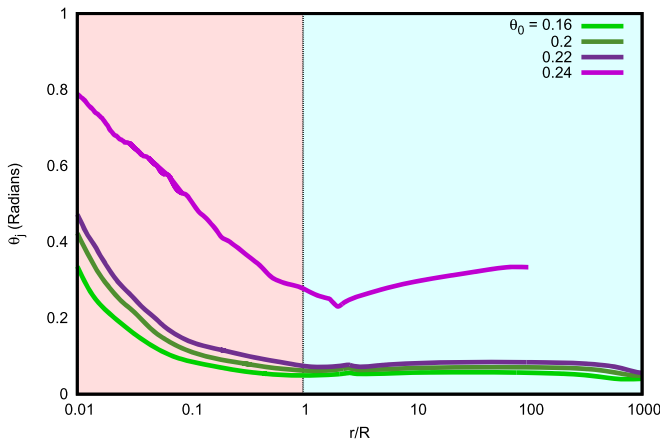


**Figure 2.** Choosing a high CSM density ( $A = 4 \times 10^{16} \text{ g cm}^{-1}$  or  $0.02M_{\odot}$  within  $10^{14} \text{ cm}$ ) and fixed GRB energy  $E = 1.4 \times 10^{51} \text{ ergs}$  but varying the injected opening angle ( $\theta_0 = 0.16, 0.2, 0.22,$  and  $0.24$ ; the final opening angle is a nonlinear function of the injection angle). All models that successfully make it out of the star do not choke or spread significantly in the CSM. Most of these jets have narrow final opening angles ( $\theta$  ranging from 0.05 to 0.08, such that  $L_{\text{iso}}$  ranges from  $2 \times 10^{52}$  to  $5 \times 10^{52} \text{ erg s}^{-1}$ ) but our widest injection has a final opening angle of 0.33, so that  $L_{\text{iso}} = 1.1 \times 10^{51} \text{ erg s}^{-1}$ .

Numerical calculations are carried out using the JET code (Duffell & MacFadyen 2011, 2013). The JET code solves the equations of relativistic gas dynamics using a moving mesh. The mesh motion allows for evolution of very high Lorentz factors over many orders of magnitude of expansion.

### 3.1. Initial Conditions

The initial conditions assume a “generic progenitor” model, identical to the stellar model used in Barnes et al. (2018). Specifically, the initial density is given by

$$\rho_{\text{init}}(r) = \begin{cases} \rho_{\text{star}}(r) + A/R_0^2 & r < R_0 \\ A/r^2 & r > R_0 \end{cases}, \quad (5)$$

where

$$\rho_{\text{star}}(r) = \frac{0.0615M_{\text{prog}}}{R_0^3} (R_0/r)^{2.65} (1 - r/R_0)^{3.5}, \quad (6)$$

$M_{\text{prog}}$  is the progenitor mass after core collapse, and  $R_0$  is the stellar radius. Fiducial values for these quantities are  $M_{\text{prog}} = 2.5M_{\odot}$  and  $R_0 = 1.6R_{\odot}$ , but because of hydrodynamical scale invariance, these values do not need to be explicitly chosen. Just as in Barnes et al. (2018), material interior to  $r < 1.5 \times 10^{-3} R_0$  is reduced significantly in density, assuming the core has collapsed and left a cavity behind.

Pressure is chosen to be initially negligible and velocity is set to zero everywhere. Note the CSM extends to infinity, and not to some finite “extended stellar radius.” Therefore, if  $A$  is sufficiently large, the jet will be choked when the engine has been turned off, regardless of how far the jet has propagated.

The engine is injected as a source term, as in Duffell & MacFadyen (2015), Barnes et al. (2018), and Duffell et al. (2018). In this study, however, the engine luminosity is a constant until the time  $t = T$ , at which point the engine is instantaneously shut off. This is to ensure that the engine shut-off occurs at a well-defined instant in time (although real GRB engines probably do not behave in this way). For our calculations, the jet power is  $L = 10^{-4}M_0c^3/R_0$ , or

$1.2 \times 10^{50} \text{ erg s}^{-1}$ . The opening angle of the engine is  $\theta_0 = 0.16$ , but the head of the jet may become narrower than this.

We perform several different calculations. First, a test run is performed where the engine is shut off before breakout from the stellar surface ( $T = 0.25R_0/c = 0.93 \text{ s}$ ), to demonstrate that the star can indeed choke the jet if the engine is shut off too soon.

Second, a suite of calculations is performed where the engine is shut off significantly after breakout from the stellar surface ( $T = 3R_0/c = 11 \text{ s}$ ), but where the external density is varied to determine how dense a CSM is necessary to choke the jet. The choices of wind parameter range from  $A = 10^{-9} M_0/R_0 = 4 \times 10^{13} \text{ g cm}^{-1}$  to  $10^{-2} M_0/R_0 = 4 \times 10^{20} \text{ g cm}^{-1}$ , with eight total choices of  $A$ , set a factor of ten apart. Our calculation with  $A = 10^{-6} M_0/R_0$  is equivalent to  $0.01M_{\odot}$  of CSM spread out over  $4 \times 10^{13} \text{ cm}$ .

Third, for our set of calculations with  $A = 10^{-6} M_0/R_0$  (the highest observed densities), we run a handful of models with the same energy and duration ( $T = 11 \text{ s}$ ) but wider injection angles ( $\theta_0 = 0.16, 0.2, 0.22,$  and  $0.24$ ), to see whether any of these jets choke or appreciably spread in the CSM.

For these tests, the total energy in the “early shut-off” model is  $1.2 \times 10^{50} \text{ erg}$ , and the total energy deposited in each of the other models is  $1.4 \times 10^{51} \text{ erg}$ .

### 3.2. Diagnostics

We measure the opening angle of the jet with time, calculated from the isotropic equivalent energy, as in Duffell & Laskar (2018). The solid angle  $\Omega$  subtended by the jet is computed by

$$\Omega = 4\pi E/E_{\text{iso}}, \quad (7)$$

which, given the following expression to compute  $E_{\text{iso}}$ ,

$$E_{\text{iso}} = 4\pi \frac{\int (dE/d\Omega)^2 d\Omega}{\int (dE/d\Omega) d\Omega} \quad (8)$$

results in the following formula for  $\theta_j$ , which is evaluated at regular intervals:

$$\sin(\theta_j/2) = \frac{E}{\sqrt{4\pi \int (dE/d\Omega)^2 d\Omega}}. \quad (9)$$

The opening angle  $\theta_j$  is measured as a function of time, to determine how much the jet widens after the engine is turned off.

## 4. Results and Discussion

Figure 1 shows opening angle as a function of forward shock radius for our suite of jet models. The “early shut-off” jet (dashed curve) begins to spread immediately after the engine is turned off, as the jet is still propagating through the star at the shut-off time; this jet is properly choked.

For the other models, as the engine is turned off after the shock has expanded to  $r > R_0$ , the jet spreading depends on the density. In particular, none of the models experienced significant spreading of the jet, except for the three highest-density calculations ( $A = 10^{-4} M_0/R_0, 10^{-3} M_0/R_0,$  and  $10^{-2} M_0/R_0$ ). In fact, as we discuss in Section 1.4, for all but the highest-density case this spreading does not appear to be due to jet “choking,” but simply the jet spreading slowly as it

**Table 1**  
Summary of Highest-density Models

$A[M_0/R_0]$	$A$ [g cm <sup>-1</sup> ]	Mass <sup>a</sup>	$\lambda/4$	$R_{RS}[R_0]$	$L_{iso}^{obs}$ [erg s <sup>-1</sup> ] <sup>b</sup>
$10^{-2}$	$4 \times 10^{20}$	$30M_\odot$	$10^0$	5.4	$4 \times 10^{50}$
$10^{-3}$	$4 \times 10^{19}$	$3M_\odot$	$10^1$	18	$3 \times 10^{51}$
$10^{-4}$	$4 \times 10^{18}$	$0.3M_\odot$	$10^2$	80	$1.4 \times 10^{53}$
$10^{-5}$	$4 \times 10^{17}$	$0.03M_\odot$	$10^3$	260	$10^{53}$
$10^{-6}$	$4 \times 10^{16}$	$0.003M_\odot$	$10^4$	740	$4 \times 10^{52}$

**Notes.** Summary of the highest-density models from Figure 1, and a measurement of the jet position at the time of reverse shock crossing ( $R_{RS}$ , near the position where the opening angle is at a minimum).

<sup>a</sup> The total wind mass within  $10^{13}$  cm.

<sup>b</sup> The observed  $L_{iso}$ , given by  $L/\theta_j^2$ , where the opening angle  $\theta_j$  is measured at  $10^{13}$  cm.

decelerates, like a standard afterglow jet. Only the highest-density CSM exhibited enough spreading to call the jet “choked.” The critical density appears to be  $A = 10^{-3} M_0/R_0 = 4 \times 10^{19}$  g cm<sup>-1</sup>, which corresponds to  $\lambda = \lambda_{crit} = 40$ . This is consistent with the prediction of Bromberg et al. (2011) for the transition between a collimated versus uncollimated jet. Such a density necessitates several solar masses of CSM within  $10^{13}$  cm of the progenitor, which is several orders of magnitude higher than any CSM density observed.

When running the suite of calculations varying the opening angle with fixed density and energy consistent with observed values (Figure 2), essentially no choking or spreading was observed for any model that was not choked before escaping the star.

#### 4.1. Comparison to Nakar (2015) Analysis

Nakar (2015) described jet breakout from the CSM in terms of the minimum engine duration necessary for a successful jet, summarized by the following inequality:

$$t_{engine} \gtrsim 150 \left( \frac{L_{iso}}{10^{51} \text{erg s}^{-1}} \right)^{-1/2} \times \left( \frac{R_{ext}}{3 \times 10^{13} \text{cm}} \right)^{1/2} \left( \frac{M_{ext}}{0.01 M_\odot} \right)^{1/2} \text{ s.} \quad (10)$$

This inequality was found by relating the outer radius of the CSM  $R_{ext}$  to the position that the jet has reached by the time the reverse shock crosses, as a function of the engine shut-off time. Another way of expressing this inequality is

$$t_{engine} \propto L_{iso}^{-1/2} R_{RS}^{1/2} M_{RS}^{1/2}, \quad (11)$$

where  $R_{RS}$  and  $M_{RS}$  are the jet position and CSM mass coordinate at the time the reverse shock crosses. As  $M_{RS} = 4\pi AR_{RS}$ , this expression can be re-written in terms of  $\lambda$ :

$$R_{RS} \propto \lambda^{1/2} t_{engine}. \quad (12)$$

Equation (10) (Nakar’s Equation (4)) follows from the assumption that if the reverse shock crosses at a radius  $R_{RS} < R_{CSM}$ , then the jet chokes in the CSM. We argue that the jet still has the opportunity to escape after the reverse shock crosses, but first we show that our results confirm

the Nakar (2015) scaling for  $R_{RS}$ , and measure the overall coefficient directly.

Table 1 shows our highest-density models and the value of  $R_{RS}$ ; the position of the jet when the reverse shock crosses (i.e., when the jet head has received the information that the engine has shut off; this is approximately the position in Figure 1 where the opening angle is narrowest, before spreading begins). Our results very precisely follow Nakar’s scaling, with the following coefficient:

$$R_{RS} = 1.3 \lambda^{1/2} c t_{engine}. \quad (13)$$

Given this coefficient of 1.3, one can derive a more accurate normalization for Equation (10), which is 30 s, rather than 150 s:

$$t_{engine} \gtrsim 0.2 \left( \frac{M_{ext} R_{ext}}{L_{iso}/c} \right)^{1/2}. \quad (14)$$

We stress that this criterion only states how long the engine needs to remain active in order that the jet escapes before the reverse shock crosses. The crossing of the reverse shock is still not a guarantee that the jet is choked.

#### 4.2. “Choked” versus Spreading

While jets do not appear to ever be rapidly “choked” in the CSM for observed CSM densities, non-choked jets can still have their opening angle widened slightly as they propagate out due to the normal spreading process typical of GRB afterglow jets. We define the distinction between “choked” and merely “spreading” by the evolution of the opening angle with time; choked jets evolve as in Irwin et al. (2019) (such jets should be roughly isotropic by the time they emerge from the dense CSM), whereas jets that are merely “spreading” evolve like GRB afterglow jets, as in Zhang & MacFadyen (2009), Granot & Piran (2012), and Duffell & Laskar (2018). In the case of jet spreading, the final opening angle has nothing to do with the duration of the engine. It only has to do with the Lorentz factor of the jet after entraining the CSM, and how this Lorentz factor compares to  $1/\theta_j$ . The Lorentz factor is given by

$$\Gamma \approx 3 \sqrt{\frac{E_{iso}}{M_{CSM} c^2}} \quad (15)$$

(Blandford & McKee 1976).

For a CSM mass of  $0.01 M_\odot$ , the final Lorentz factor can range from 1 to 50, depending on  $E_{iso}$ . Jets that attain low-Lorentz factors will still require a few orders of magnitude of expansion to spread (Zhang & MacFadyen 2009; Duffell & Laskar 2018), so this low-Lorentz factor must be attained early in order to significantly change the jet opening angle. Typically, non-choked jets stay reasonably narrow ( $\theta_j < 20^\circ$ ) until they decelerate to nonrelativistic velocities (see Figure 1 of Duffell & Laskar 2018). Thus, only the very weakest GRB jets with  $E_{iso} \sim 10^{51}$  erg could widen significantly via spreading in the CSM, independent of the duration of the engine.

For reference, the run that exhibited spreading to 0.4 radians in Figure 1 has  $E_{iso}/(M_{CSM} c^2) = 0.03$  (where  $E_{iso}$  was computed before spreading), comparable to a very low-energy GRB with  $E_{iso} = 10^{51}$  erg in  $0.01 M_\odot$  of CSM. So, if spreading occurs it will only be for the lowest-energy jets in the highest-

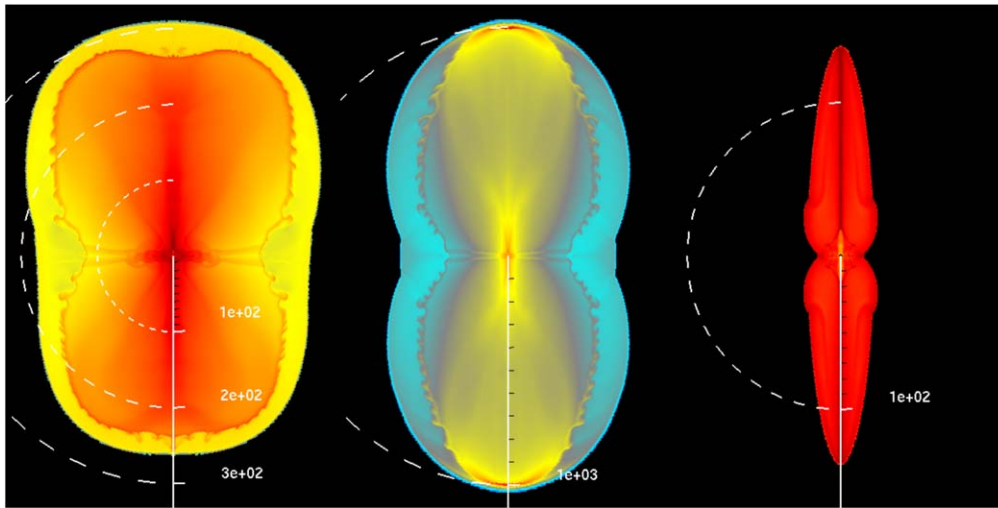


**Figure 3.** Energy density in several different models, long after breakout from the star, and long after the engine is shut off;  $t = 10^3 R_0 / c \approx 1$  hr. All models have been interacting with the CSM for the entire hour after breakout. Left: The “Early Shut-Off” model, properly choked before escaping the star. The outflow is more spherical and sub-relativistic; the forward shock is only propagating at about  $0.25c$ . Center: A low-density CSM model ( $A = 10^{-9} M_0 / R_0$ ) whose engine was shut off after breakout; the CSM density was not high enough to choke the jet. The jet is narrow and relativistic ( $\Gamma = 285$ ). Right: A jet which was somewhat choked by the CSM ( $v = 0.25c$ ). The jet core is still collimated but a large portion of the energy is more spherically distributed, at low velocities. This required a very high density;  $A = 10^{-2} M_0 / R_0 \approx 4 \times 10^{20} \text{ g cm}^{-1}$ .

density CSM, and even in this case the spreading is quite modest, as the final opening angle is about  $20^\circ$ .

#### 4.3. Possible Connection to Afterglow Plateaus

Even if the jet is not choked, it may entrain a significant amount of mass, decelerating it to a lower Lorentz factor than it emerged with from the star. For example, a typical jet will sweep up 1% of the surrounding CSM, which for a  $10^{51}$  erg jet in a  $0.01 M_\odot$  CSM, results in a jet Lorentz factor of  $\Gamma \sim 10$  upon emerging from the CSM. This jet could still remain somewhat collimated until it swept up significant mass during the afterglow phase. This would give rise to a long plateau as the jet coasts at a modest Lorentz factor, similar to the “top-heavy” plateau model of Duffell & MacFadyen (2014). According to that study, the deceleration time (according to the observer) is sensitive to the Lorentz factor:

$$t_{\text{decel}}^{\text{obs}} \sim \frac{E_{\text{iso}}}{\rho_{\text{ext}} r^2 c^3 \Gamma^4} \sim \frac{10^{10} \text{ s}}{\Gamma^4}, \quad (16)$$

where  $\rho_{\text{ext}}$  is the (presumably much lower) CSM density at larger radii.

If the jet emerges from the dense component of the CSM with a Lorentz factor  $\Gamma \approx 10$ , this could lead to a plateau duration of up to  $10^6$  s, as long as several days. In practice, many CSM environments may not be this dense, only decelerating the jet to a Lorentz factor of 30 or so, leading to more modest plateau durations.

One way of confirming this scenario would be to make observations of the reverse shock during the afterglow, to measure the Lorentz factor of the jet during the plateau (Laskar et al. 2013; Alexander et al. 2017). So far, the handful of direct observations of reverse shocks have all coincided with afterglows that did not exhibit an X-ray plateau. Similarly, one would expect (for the same CSM mass) that the plateau

duration should be inversely proportional to  $E_{\text{iso}}$ :

$$t_{\text{decel}}^{\text{obs}} \propto \frac{M_{\text{CSM}}^2 c}{\rho_{\text{ext}} r^2 E_{\text{iso}}}. \quad (17)$$

This could be a partial explanation for the observed Dainotti relation (Dainotti et al. 2008) where the luminosity of the afterglow at the end of the plateau correlates inversely with the plateau duration.

#### 4.4. Implications for the Prompt Emission

A “non-choked” jet might still be unobservable if it is sufficiently decelerated before gamma-rays can be emitted. In this case, it is possible that a very dense CSM might hide the burst sufficiently well that it effectively does not matter whether the jet was choked. Such a jet would still produce an afterglow, but without the prompt emission it would be much harder to detect (but see Berger et al. 2013; Cenko et al. 2013, 2015; Ho et al. 2018). Alternatively, it is possible that this still produces a low-luminosity GRB via shock breakout, similar to what was predicted by Nakar (2015), but in contrast with that picture, the shock energy would not be redistributed spherically; it would still be concentrated in the direction of the jet.

However, for a modestly dense CSM (say, a few times  $10^{-3} M_\odot$ ) or a high-energy jet ( $E_{\text{iso}} \sim 10^{54}$  erg), it might be possible to produce a soft GRB (or X-ray burst) coupled with an afterglow exhibiting a long plateau. This is very similar to the “dirty fireball” model of Dermer et al. (2000). However, in that model, the jet is thought to entrain material within the star itself. Such a GRB produced by a low-Lorentz factor jet would be expected to have a much longer than typical variability timescale (or no variability at all), as some of the strongest evidence for high Lorentz factors comes from the rapid variability timescales typically seen.

A potentially observable signature would be a correlation between soft or low-variability GRBs and longer plateaus in the afterglow (and if a reverse shock is observed, a modest

Lorentz factor for the jet). If this dense CSM were responsible for most X-ray plateaus, one would expect afterglows with long plateaus to exhibit lower  $E_{\text{iso}}$  and longer-time variability in the prompt emission than afterglows without plateaus. This motivates a search for a connection between afterglow plateau properties and the prompt variability, to see whether such a population of “decelerated but not choked” jets exists.

We thank Tanmoy Laskar, Kate Alexander, Edo Berger, and Andrew MacFadyen for helpful comments and discussions. We especially thank Ehud Nakar for very detailed comments and suggestions for additional calculations that have helped to bolster our arguments.

We also would like to thank the anonymous referee for the very detailed and thoughtful review, and for the suggestion of the analytic comparison with the Nakar (2015) reverse shock formula (Section 4.1).

Initial interactions between the coauthors were facilitated by the ZTF theory network, which is funded by the Gordon and Betty Moore Foundation through Grant GBMF5076.

High-resolution calculations were provided by the NASA High-End Computing (HEC) Program through the NASA Advanced Supercomputing (NAS) Division at Ames Research Center.

P.C.D. is supported by Harvard University through the ITC Fellowship. A.Y.Q.H. is supported by a National Science Foundation Graduate Research Fellowship under grant No. DGE-1144469. This work was supported by the GROWTH project funded by the National Science Foundation under PIRE grant No. 1545949.

#### ORCID iDs

Paul C. Duffell  <https://orcid.org/0000-0001-7626-9629>  
 Anna Y. Q. Ho  <https://orcid.org/0000-0002-9017-3567>

#### References

- Alexander, K. D., Laskar, T., Berger, E., et al. 2017, *ApJ*, 848, 69  
 Barnes, J., Duffell, P. C., Liu, Y., et al. 2018, *ApJ*, 860, 38  
 Berger, E., Leibler, C. N., Chornock, R., et al. 2013, *ApJ*, 779, 18  
 Blandford, R. D., & McKee, C. F. 1976, *PhFI*, 19, 1130  
 Bromberg, O., Nakar, E., Piran, T., & Sari, R. 2011, *ApJ*, 740, 100  
 Campana, S., Mangano, V., Blustin, A. J., et al. 2006, *Natur*, 442, 1008  
 Cano, Z., Wang, S.-Q., Dai, Z.-G., & Wu, X.-F. 2017, *AdAst*, 2017, 8929054  
 Cenko, S. B., Kulkarni, S. R., Horesh, A., et al. 2013, *ApJ*, 769, 130  
 Cenko, S. B., Urban, A. L., Perley, D. A., et al. 2015, *ApJ*, 803, L24  
 Corsi, A., Ofek, E. O., Gal-Yam, A., et al. 2014, *ApJ*, 782, 42  
 Dainotti, M. G., Cardone, V. F., & Capozziello, S. 2008, *MNRAS*, 391, L79  
 Dermer, C. D., Chiang, J., & Mitman, K. E. 2000, *ApJ*, 537, 785  
 Duffell, P. C., & Laskar, T. 2018, *ApJ*, 865, 94  
 Duffell, P. C., & MacFadyen, A. I. 2011, *ApJS*, 197, 15  
 Duffell, P. C., & MacFadyen, A. I. 2013, *ApJ*, 775, 87  
 Duffell, P. C., & MacFadyen, A. I. 2014, *ApJL*, 791, L1  
 Duffell, P. C., & MacFadyen, A. I. 2015, *ApJ*, 806, 205  
 Duffell, P. C., Quataert, E., Kasen, D., & Klion, H. 2018, *ApJ*, 866, 3  
 Filippenko, A. V. 1997, *ARA&A*, 35, 309  
 Granot, J., & Piran, T. 2012, *MNRAS*, 421, 570  
 Ho, A. Y. Q., Goldstein, D. A., Schulze, S., et al. 2019, *ApJ*, 887, 169  
 Ho, A. Y. Q., Kulkarni, S. R., Nugent, P. E., et al. 2018, *ApJ*, 854, L13  
 Irwin, C. M., Nakar, E., & Piran, T. 2019, *MNRAS*, 489, 2844  
 Izzo, L., de Ugarte Postigo, A., Maeda, K., et al. 2019, *Natur*, 565, 324  
 Laskar, T., Berger, E., Zauderer, B. A., et al. 2013, *ApJ*, 776, 119  
 MacFadyen, A. I., Woosley, S. E., & Heger, A. 2001, *ApJ*, 550, 410  
 Margutti, R., Guidorzi, C., Lazzati, D., et al. 2015, *ApJ*, 805, 159  
 Mészáros, P., & Waxman, E. 2001, *PhRvL*, 87, 171102  
 Modjaz, M., Liu, Y. Q., Bianco, F. B., & Graur, O. 2016, *ApJ*, 832, 108  
 Nakar, E. 2015, *ApJ*, 807, 172  
 Nakar, E. 2019, *Natur*, 565, 300  
 Nakar, E., & Piro, A. L. 2014, *ApJ*, 788, 193  
 Piro, A. L. 2015, *ApJ*, 808, L51  
 Salas, P., Bauer, F. E., Stockdale, C., & Prieto, J. L. 2013, *MNRAS*, 428, 1207  
 Sobacchi, E., Granot, J., Bromberg, O., & Sormani, M. C. 2017, *MNRAS*, 472, 616  
 Soderberg, A. M., Chevalier, R. A., Kulkarni, S. R., & Frail, D. A. 2006, *ApJ*, 651, 1005  
 Terreran, G., Margutti, R., Bersier, D., et al. 2019, *ApJ*, 883, 147  
 Whitesides, L., Lunnan, R., Kasliwal, M. M., et al. 2017, *ApJ*, 851, 107  
 Woosley, S. E., & Bloom, J. S. 2006, *ARA&A*, 44, 507  
 Zhang, W., & MacFadyen, A. 2009, *ApJ*, 698, 1261